A Generalized Coupling Matrix Extraction Technique for Bandpass Filters With Uneven-Qs

Hai Hu, *Student Member, IEEE*, and Ke-Li Wu, *Fellow, IEEE*

***Abstract*—In this paper, a vector fitting (VF) based analytical extraction method, which is capable of accurately extracting the coupling matrix and the uneven unloaded Qs of each electric resonators of a filter, is presented. Having had the complex poles and residues determined using VF, the coupling matrix can be obtained by a sequence of complex orthogonal transformations. As a side product, the unloaded Qs for each resonator will be directly obtained from the complex diagonal elements of the coupling matrix. To demonstrate the effectiveness of the proposed method, an ideal demonstrative example along with two practical challenging filter tuning examples, namely, an eight-pole dual-mode dielectric filter and an eight-pole dual-mode predistortion filter, are demonstrated. An excellent match between the responses of the measured data and those from the extracted coupling matrix with actual unloaded Q factors can be seen.**

***Index Terms*—Computer-aided tuning (CAT), coupling matrix, filters, predistortion filter.**

I. Introduction

MICROWAVE filters are indispensible components in every communication system. They are not only used for transmitters and receivers, but also used in various multiplexer sub-systems for channelizing a broadband microwave signal. Among different type of filters, narrowband bandpass filters (fractional bandwidth, or $\mathrm{FBW} < 5\%$) are most widely used in various communication infrastructure systems, such as the radio units in wireless base stations and input/output multiplexers on communication satellites. In order to meet the increasingly stringent selectivity requirement, many narrowband filters are high-order general Chebshev types incorporating multiple cross-couplings [1]. To compensate the manufacture tolerance and the inaccurate dimension design, the production of such narrowband filters heavily depends on manual tunings. It is highly desirable that such human tuning built up by experience be replaced by a computer-aided procedure through the extraction of a filter circuit model, which is commonly expressed by a coupling matrix [2].

Manuscript received August 16, 2013; revised December 13, 2013; accepted December 18, 2013. Date of publication January 09, 2014; date of current version February 03, 2014. This work was supported by the University Grants Committee, Hong Kong Special Administrative Regionunder Grant AoE/P-04/08.

H. Hu was with the Department of Electronic Engineering, The Chinese University of Hong Kong, Shatin NT, Hong Kong. He is now with the Asia Satellite Telecommunications Company Ltd., Hong Kong.

K.-L. Wu with the Department of Electronic Engineering, The Chinese University of Hong Kong, Shatin NT, Hong Kong (e-mail: klwu@ee.cuhk.edu.hk).

Color versions of one or more of the figures in this paper are available online at http://ieeexplore.ieee.org.

Digital Object Identifier 10.1109/TMTT.2013.2296744

Computer-aided tuning (CAT) technology for microwave filters was originally developed for the tuning of dual-mode filters [3]. Since then, the technology has been widely adopted by the filter industry, as it provides an efficient means for filter tuning in a deterministic way without requiring too much experience. The most critical process in CAT is to diagnose (or extract) the circuit model corresponding to a measured microwave filter response from severely detuned to well-tuned states. It is well understood for a filter designer that for a bandpass filter, the nonzero entries in its coupling matrix have their one-to-one correspondence to the tuning and coupling elements in a filter physical realization. By comparing the extracted coupling matrix with the target coupling matrix, the tuning direction and the amount of physical adjustment can be decided for each tuning element at each tuning state. The CAT technique is very useful in tuning advanced microwave bandpass filters such as high-order filters with cross couplings or singly terminated channel filters whose responses are not well matched [4]. Toward this end, many effective CAT algorithms have been proposed for different scenarios [3], [5]–[9], among which an analytical extraction approach for a filter with high and nearly even unloaded Q factors was presented in [9].

It is a common sense that the insertion loss for a narrow bandpass filter is inevitable and is contributed by unevenly distributed losses among filter resonators, which are described by the uneven unloaded Qs of each resonator. The uneven Qs can be caused by intentional factors, such as mixed modes/types of resonators [10], and unintentional factors, such as unequal penetration depths of tuning screws in each resonator. When the uneven-Q phenomenon becomes prominent, it will be difficult for the existing techniques to extract a correct circuit model. Therefore, to accurately reflect the loss effect for a general filter case, a generalized extraction algorithm that is capable of handling uneven Q factors needs to be developed.

One practical application of the generalized extraction algorithm is the tuning of a predistortion filter. A predistortion filter [11]–[14], which can have a very high effective Q factor in terms of the flatness of insertion loss and the sharpness of selectivity, has been recently adopted in the input multiplexer (IMUX) of a communication satellite payload system [12]. This technology allows the use of much smaller sized lossy resonators so that the overall mass of the payload can be reduced significantly. Nevertheless, the design of a predistortion filter that can achieve the prescribed insertion-loss flatness with the minimal absolute insertion-loss level requires the knowledge of the Q factor for each resonator. The tuning process of such a filter is much more challenging than the tuning of an ordinary filter because the couplings and Q factors of the lossy resonators used are more sensitive to the tuning screws' adjustment. Therefore, the uneven-Q effect must be taken into account in the design and tuning process of a predistortion filter.

Generally speaking, all practical microwave bandpass filters exhibit an uneven-Q effect to a certain degree. However, the existing extraction methods cannot effectively and accurately handle such an effect. The optimization-based methods such as those in [3] and [5]–[7] may not be a good choice unless good quality initial values to the coupling matrix, phase loadings, and the Q factors can be given. The analytical extraction methods such as those in [8] and [9], on the other hand, do not effectively handle the uneven-Q effect either. In [8], a uniform Q distribution is assumed. While the method proposed in [9], which is based on the Y-parameter fractional expansions, can be effective for lossless and nearly even-Q filters. However, [9] may fail to deal with very lossy and detuned filters because the system poles may not be easily distinguished from the magnitude information of Y-parameters. A decisive limiting factor in [9] is that the imaginary part of the system poles of the Y-parameters, which determine the resonators' Q factors, are derived based on the assumption of pure real system residues. This assumption is not true for a general filter with uneven Qs. In fact, the constant filter Q factor defined in a filter synthesis process is valid only when the filter has a relatively equal loss distribution among all the resonators.

In this paper, a generalized analytical extraction method that deals with lossy filters with unevenly distributed Q factors is presented. This method is based on the filter admittance parameter response. The vector fitting (VF) [16], [17] algorithm, which is widely used to rationalize a linear system, is exploited to extract the complex system poles and residues. The use of VF algorithm for extracting filter circuit model was also briefly reported in [18]. In that work, the residues of Y-parameter fractional expansions are assumed to be real and the real part of the complex poles are used to calculate an approximated constant Q factor from only an electromagnetic (EM) simulated filter response. However, in this paper, VF is used to tackle the general practical filter case and the uneven-Q effect is fully considered in the obtained circuit model. With the proposed method, the actual loss of a physical filter model is represented by the extracted Q factors of each resonator. It will be demonstrated through two challenging hardware filter tuning examples that the proposed method is a robust and versatile tool for CAT of advanced bandpass filters.

II. Finding Complex System Poles and Residues Using VF Method

It has been shown in [9] that before extracting a coupling matrix from a measured filter response, a constant phase loading and any embedded transmission line must be removed. This is because the filter circuit model described by a coupling matrix does not incorporate any embedded transmission line or a constant phase shift (phase loading) at the ports, which, however, always exists in a filter physical model. After the extra phase effects being accurately removed, the filter Y-parameter poles and residues can be found correctly to restore the coupling matrix.

Previously in [9], the system poles are determined from the magnitudes of Y-parameters. However, this method is not reliable when the filter loss is large and the peaks become too blunt to be distinguished.

In this extraction algorithm, VF is adopted to determine the system poles and zeros (or residues). VF is a popular tool for system identification of a linear system [16], [17]. VF rationalizes a system with guaranteed stable poles by iteratively identifying the system poles and zeroes. For the readers' convenience, the core procedure of VF method is briefly reviewed here.

In order to rationalize a measured system $Y(s)$ by a rational function with N system poles

$$Y(s) = \sum_{i=1}^{N} \frac{c_i}{s - a_i} + d \tag{1}$$

where a_i, c_i, and d are actual poles, residues and leading constant of $Y(s)$, respectively, a set of initial poles $\bar{a}_i, i = 1, \ldots N$, located at arbitrary complex frequencies, are assumed first.

Defining an auxiliary function $\sigma(s)$,

$$\sigma(s) = \sum_{i=1}^{N} \frac{\bar{c}_i}{s - \bar{a}_i} + 1 \tag{2}$$

whose product with $Y(s)$, denoted by $W(s)$, is enforced to approximate the system by

$$W(s) = \sigma(s)Y(s) = \sum_{i=1}^{N} \frac{c_i}{s - \bar{a}_i} + d. \tag{3}$$

Substituting (2) into (3) yields

$$\sigma(s)Y(s) = \left(\sum_{i=1}^{N} \frac{\bar{c}_i}{s - \bar{a}_i} + 1\right) Y(s) = \sum_{i=1}^{N} \frac{c_i}{s - \bar{a}_i} + d \tag{4}$$

which can be rearranged to

$$\sum_{i=1}^{N} \frac{c_i}{s - \bar{a}_i} + d - \sum_{i=1}^{N} \frac{\bar{c}_i}{s - \bar{a}_i} Y(s) = Y(s). \tag{5}$$

Since $\bar{a}_i$ is known, the rest of coefficients c_i, d and $\bar{c}_i$ can be found from (5) by sampling (5) at multiple frequency points s_k and solving a linear least square (LS) problem

$$Ax = b \tag{6}$$

where

$$x = [c_1, \ldots, c_N, d, \bar{c}_1, \ldots, \bar{c}_N]^T \tag{7}$$

and the kth row of A and b are

$$\begin{aligned} A_k &= \left[\frac{1}{s_k - \bar{a}_1}, \ldots, \frac{1}{s_k - \bar{a}_N}, 1, \frac{-Y(s_k)}{s_k - \bar{a}_1}, \ldots, \frac{-Y(s_k)}{s_k - \bar{a}_N}\right] \\ b_k &= Y(s_k). \end{aligned} \tag{8}$$

Having found the unknowns in (6), $\sigma(s)$ and $W(s)$ can be transformed into their pole-zero forms

$$W(s) = d\prod_{i=1}^{N}\frac{s-z_i}{s-\bar{a}_i} \tag{9}$$

$$\sigma(s) = \prod_{i=1}^{N}\frac{s-\bar{z}_i}{s-\bar{a}_i}. \tag{10}$$

According to (3), $Y(s)$ can then be expressed by

$$Y(s) = \frac{W(s)}{\sigma(s)} = d\prod_{i=1}^{N}\frac{s-z_i}{s-\bar{z}_i}. \tag{11}$$

It can be observed that the new poles of $Y(s)$ are actually the zeroes of $\sigma(s)$ instead of the initial poles. This pole-zero calculation process can be repeated by starting from (2) and (3) with $\bar{z}_i$ in (11) as the initial poles in a new iteration. When the solution converges, the finally determined poles $\bar{z}_i$ must be the same as the actual poles a_i, as is stated in (1).

The VF method possesses the following distinct advantages:

1) highly reliable for lossy and detuned high-order filters;
2) network parameters Y_{11}, Y_{21}, and Y_{22} of a filter can be rationalized by one run;
3) iterative fitting process converges rapidly.

It should be noted that the complex system poles and residues vector fitted from a filter bandpass response are in conjugate pairs and the system order is twice as that of the filter. However, only the poles with a positive imaginary part (and the associated residues) are then transformed to low-pass domain in which the coupling matrix is defined.

III. Filter Circuit Model With Uneven Q Factors

In most analytical extraction theories [8], [9], [18], a uniform Q factor for all resonators of a filter is assumed. In this case, the system residues must be real numbers. However, it will be shown in this section that for a filter with uneven Qs, not only the poles, but also the residues, must be complex values. Based on this observation, the CAT method presented in this paper can then be greatly enhanced to handle the filter with uneven Qs.

A typical microwave bandpass lossy filter can be expressed by a mutually coupled *RLC* loop circuit network, as is shown in Fig. 1(a). The filter bandpass prototype can be transformed to its equivalent low-pass prototype, as is shown in Fig. 1(b), which is described by an $N+2$ coupling matrix [15].

To analyze a coupled-resonator filter with the general $N+2$ coupling matrix model as shown in Fig. 1(b), its circuit loop equations can be written as [15]

$$e_g[1,0,\ldots,0]^T = [j\boldsymbol{M} + s\boldsymbol{I} + \boldsymbol{R}][i_S, i_1, \ldots, i_N, i_L]^T \tag{12}$$

where e_g is the voltage of the source, $\boldsymbol{M}$ is the $N+2$ coupling matrix, $i_S, i_1, \ldots, i_N, i_L$ are the loop currents for the $N+2$ loops, s is the complex angular frequency in the low-pass domain, $\boldsymbol{I}$ is an $N+2$ by $N+2$ diagonal matrix

$$\boldsymbol{I} = \mathrm{diag}(0,1,1,\ldots,1,0) \tag{13}$$

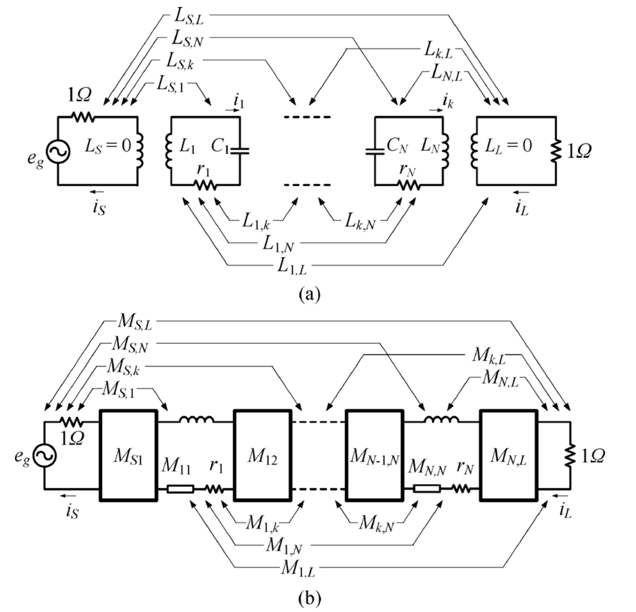

Fig. 1. Coupled-resonator microwave filter with loss. (a) Bandpass prototype with *RLC* loops. (b) Equivalent low-pass prototype, which is described by an $N+2$ coupling matrix.

and $\boldsymbol{R}$ contains the loss terms of the $N+2$ loops and the unit termination impedances

$$\boldsymbol{R} = \mathrm{diag}(1, r_1, r_2, \ldots, r_N, 1) \tag{14}$$

The matrix equation (12) can be further rearranged as

$$\begin{bmatrix}\boldsymbol{V_p}\\ 0\end{bmatrix} = \begin{bmatrix}0 & 0\\ 0 & \boldsymbol{S}\end{bmatrix}\begin{bmatrix}\boldsymbol{I_p}\\ \boldsymbol{i}\end{bmatrix} + j\begin{bmatrix}\boldsymbol{C} & \boldsymbol{b^T}\\ \boldsymbol{b} & \boldsymbol{M'}\end{bmatrix}\begin{bmatrix}\boldsymbol{I_p}\\ \boldsymbol{i}\end{bmatrix} \tag{15}$$

in which

$$\boldsymbol{V_p} = \begin{bmatrix}v_S\\ v_L\end{bmatrix} = \begin{bmatrix}e_g - i_S\\ -i_L\end{bmatrix} \quad \boldsymbol{I_p} = \begin{bmatrix}i_S\\ i_L\end{bmatrix} \quad \boldsymbol{i} = \begin{bmatrix}i_1\\ \vdots\\ i_N\end{bmatrix} \tag{16}$$

are the port voltages, port currents, and the internal loop currents, respectively. The general $N+2$ coupling matrix $\boldsymbol{M}$ is rearranged in the second term on the right-hand side of (15), where

$$\boldsymbol{M'} = \begin{bmatrix} M'_{11} & M_{12} & \cdots & M_{1N}\\ M_{21} & M'_{22} & \cdots & M_{2N}\\ \vdots & \vdots & \ddots & \vdots\\ M_{N1} & M_{N2} & \cdots & M'_{NN}\end{bmatrix} \tag{17}$$

is the core N by N coupling matrix of the filter with the loss terms added on the diagonal

$$M'_{k,k} = M_{k,k} - j\frac{f_0}{BW}\frac{1}{Q_k} \tag{18}$$

where f_0 and BW are the center frequency and bandwidth of the filter, Q_k is the unloaded Q factor for the kth resonator.

The sub-matrices $\boldsymbol{C}$ and $\boldsymbol{b}$ in (15) are the couplings associated to the source and load loops

$$\boldsymbol{C} = \begin{bmatrix} 0 & M_{\mathrm{SL}} \\ M_{\mathrm{SL}} & 0 \end{bmatrix} \quad \boldsymbol{b} = \begin{bmatrix} M_{S1} & M_{S2} & \cdots & M_{SN} \\ M_{L1} & M_{L2} & \cdots & M_{LN} \end{bmatrix}^{T}. \tag{19}$$

The complex angular frequency variable is expressed in matrix form in (15),

$$\boldsymbol{S} = sI = j\omega I \tag{20}$$

where I is an N by N identity matrix.

Since $\boldsymbol{M}'$ is a symmetric complex matrix, it can be eigen-decomposed by

$$\boldsymbol{M}' = \boldsymbol{U}\boldsymbol{\Lambda}\boldsymbol{U}^{-1} \tag{21}$$

and

$$\boldsymbol{\Lambda} = \mathrm{diag}(\lambda_1, \lambda_2, \ldots \lambda_N) \tag{22}$$

where $\lambda_1, \lambda_2, \ldots, \lambda_N$ are the system poles and $\boldsymbol{U}$ contains the corresponding eigenvectors. Since $\boldsymbol{M}'$ in general is not Hermitian (unless a lossless case is assumed), then $\boldsymbol{\Lambda}$ must be *complex* [21]. Furthermore, since $\boldsymbol{M}'$ is complex, but generally not normal (unless a constant-Q case is assumed), then $\boldsymbol{U}$ must be a nonunitary *complex* matrix [21].

From the definition of $\boldsymbol{V_p} = \boldsymbol{Y}\boldsymbol{I_p}$, the Y-parameter matrix of the two-port filter network can be obtained from (15) by

$$\boldsymbol{Y} = j\boldsymbol{C} + \boldsymbol{b}^T\boldsymbol{U}(\boldsymbol{S} + j\boldsymbol{\Lambda})^{-1}\boldsymbol{U}^{-1}\boldsymbol{b}. \tag{23}$$

Denoting $\boldsymbol{g} = \boldsymbol{b}^T\boldsymbol{U}$ and $\boldsymbol{h} = (\boldsymbol{U}^{-1}\boldsymbol{b})^T$, the admittance matrix $\boldsymbol{Y}$ can be expressed in a fractional expansion form

$$\boldsymbol{Y} = j\boldsymbol{C} + \begin{bmatrix} \displaystyle\sum_{k=1}^{N} \frac{g_{1,k}h_{1,k}}{s + j\lambda_k} & \displaystyle\sum_{k=1}^{N} \frac{g_{1,k}h_{2,k}}{s + j\lambda_k} \\ \displaystyle\sum_{k=1}^{N} \frac{g_{2,k}h_{1,k}}{s + j\lambda_k} & \displaystyle\sum_{k=1}^{N} \frac{g_{2,k}h_{2,k}}{s + j\lambda_k} \end{bmatrix} \tag{24}$$

or

$$\boldsymbol{Y} = j\boldsymbol{C} + \sum_{k=1}^{N} \frac{1}{s + j(p_k + jq_k)} \times \begin{bmatrix} r_{11k} + jx_{11k} & r_{21k} + jx_{21k} \\ r_{21k} + jx_{21k} & r_{22k} + jx_{22k} \end{bmatrix} \tag{25}$$

where $(p_k, q_k), (r_{11\,k}, x_{11\,k}), (r_{21\,k}, x_{21\,k})$, and $(r_{22\,k}, x_{22\,k})$ are the real and imaginary parts of $\lambda_k, g_{1,k}h_{1,k}, g_{1,k}h_{2,k}$, and $g_{2,k}h_{2,k}$ of (24), respectively.

If Q factors for each resonator are assumed to be different, the diagonal matrix $\boldsymbol{\Lambda}$ and its eigenvector matrix $\boldsymbol{U}$ in (21) must be complex. That is to say, the system poles and residues in (24) are all complex numbers in general. This fact is more clearly emphasized in (25). It can be shown that if the network is lossless or the loss is uniformly distributed among resonators, the residues in (25) will become purely real.

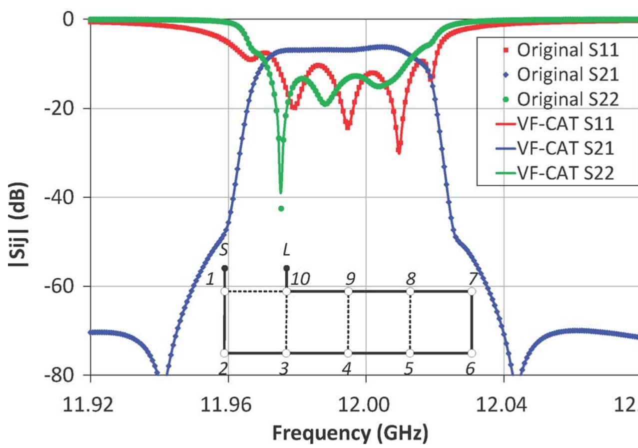

Fig. 2. Ideal ten-pole filter in Pfitzenmaier coupling topology with unequal Q factors and detuned resonators. The dotted lines are the original responses of the circuit model and the solid lines are from the VF-based extraction.

IV. Coupling Matrix in Transversal Topology

To extract the coupling matrix of an N-pole filter from measured S-parameters, the measured data will be converted to Y-parameters first. The VF method outlined in Section II is used to find the poles and residues of the Y-parameters. A transversally coupled $N + 2$ filter network [15] can then be directly restored based on the poles and residues found in (25) by

$$\begin{aligned} \bar{M}_{kk} &= M_{kk} + jX_{kk} = -p_k - jq_k, \\ \bar{M}_{Lk} &= M_{Lk} + jX_{Lk} = \sqrt{r_{22k} + jx_{22k}}, \\ \bar{M}_{Sk} &= M_{Sk} + jX_{Sk} = (r_{21k} + jx_{21k})/\sqrt{r_{22k} + jx_{22k}}, \\ & k = 1, 2, \ldots, N \end{aligned} \tag{26}$$

where $\bar{M}_{kk}$, $\bar{M}_{Sk}$, and $\bar{M}_{Lk}$ are the self-couplings, couplings between a resonator and the source or the load, respectively. Different from the conventional $N + 2$ coupling matrix [15], now all the couplings (except for M_{SL}) are complex values in general to account for a general resonator-coupled filter with uneven Qs. For a fully canonical filter, the source–load coupling M_{SL} stays real and will not be affected by the uneven-Q effect or the followed transformations.

Obviously, the complex coupling values of the off-diagonal elements for a filter are not physically realizable. However, the finally achieved coupling matrix must correspond to the actual filter's physical coupling topology. Therefore, the obtained transversal coupling matrix must be further transformed to the targeted topology through a series of complex rotations (matrix similarity transformation processes) [13], resulting in the final coupling matrix in the actual filter's coupling topology, in which the dominant loss is distributed on the diagonal terms in a correct order to reflect the true uneven Qs of each individual resonator, and the loss on off-diagonal elements becomes considerably small and is neglected.

V. Demonstrative Example: Ideal Filter With Uneven Q Factors

In this section, extraction of the coupling matrix and uneven Qs from the simulated responses of a detuned filter circuit model is demonstrated. This example is a ten-pole Pfitzenmaier filter

TABLE I
EXTRACTED UNLOADED Q FACTORS FOR EACH RESONATOR OF THE TEN-POLE FILTER

	Q1	Q2	Q3	Q4	Q5	Q6	Q7	Q8	Q9	Q10
Prescribed	1000	3000	5000	7000	9000	1000	3000	5000	7000	9000
VF-CAT	1000	3000	5000	7000	9000	1000	3000	5000	7000	9000
CAT in[9]	2425	2335	2633	2876	2663	2663	2897	3077	3595	3256

[15], whose coupling topology is illustrated in Fig. 2. The filter has $f_0 = 12$ GHz and $BW = 50$ MHz, and realizes four imaginary and four complex transmission zeros (TZs). To extract the filter circuit model, the following general steps are taken:

Step 1) deembedding the phase loading effects from the filter responses;

Step 2) determining the complex system poles and complex residues from the Y-parameters in bandpass domain by VF;

Step 3) transforming the filter system poles and residues to their low-pass counterparts;

Step 4) assembling an $N+2$ complex transversal coupling matrix directly from the low-pass system poles and residues;

Step 5) reconfiguring the transversal coupling matrix to the required coupling topology by a series of complex rotations.

In this ideal circuit model extraction example, the complex poles and residues are easily obtained from the filter responses through the aforementioned procedure. Consequently, a complex transversal coupling matrix is assembled through (26). To achieve the circuit model that corresponds to the predefined coupling topology, a series of complex matrix rotations must be performed. The rotation angles for annihilating specified matrix entries are now complex values.

It should be cautious that for certain coupling topologies, such as cascade-quartet (CQ), cascade-trisection (CT), extended box [15], etc., there is more than one rotation solution that corresponds to the initial transversal coupling matrix. In order to lock up a unique coupling matrix that matches the filter physical model in the extraction process, several key physical coupling elements, such as the widths of irises in a waveguide filter, can be accurately realized beforehand and kept fixed during the tuning process so that the corresponding coupling values in the extracted models can be used as a gauge to rule out the unwanted multiple solutions. However, this issue is not the main concern of this paper, where only the filters in the *folded* and *Pfitzenmaier* coupling topologies are considered.

The unloaded Q factors calculated from the imaginary part (only appears on the diagonal elements) of the coupling matrix after complex reconfiguration are listed in the second row of Table I, which are identical to those originally prescribed. The responses from the finally achieved filter circuit model are superimposed in Fig. 2 via solid lines, and clearly they are coincident with the original responses. For comparison purposes, the Q factors extracted using the approach with real residues [9] are given in the last row of Table I, which obviously are not correct.

Even though the extreme uneven-Q distribution case in this proof-of-concept example is rare, the proposed procedure for obtaining the correct circuit model from the complex system poles and residues has been demonstrated.

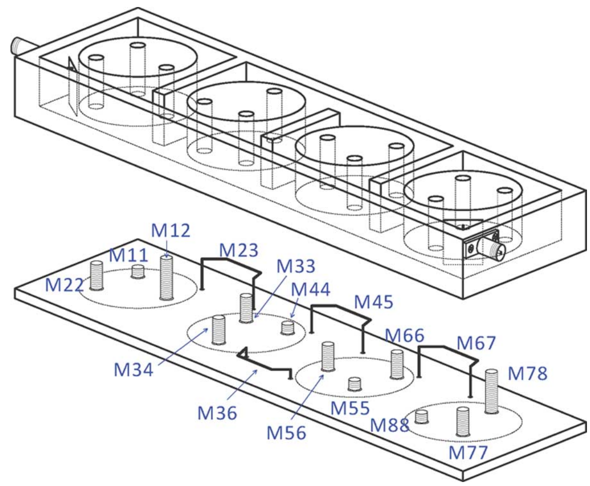

Fig. 3. Illustration of the eight-pole TM_{11} dual-mode DR filter hardware. (*top*) Filter body. (*bottom*) Filter lid with tuning screws and coupling loops, whose corresponding coupling values are also marked.

VI. PRACTICAL EXAMPLES

In this section, two practical examples are given to further demonstrate the effectiveness of the VF-based extraction method. Different from the ideal filter example, measurement noises, dispersion effect, and unwanted stray couplings are confronted in addition to the unevenly distributed Q factors.

Example 1: Tuning of an Eight-Pole Dual-Mode Dielectric Filter

This type of filter is first reported in [19], where the TM dual-mode dielectric (DR) puck with both ends short circuited to the housing cavity walls is used. This eight-pole filter is illustrated in Fig. 3, the filter center frequency and bandwidth are $f_0 = 1.949$ GHz and $BW = 62$ MHz, respectively. The DR material used has a relative permittivity of $\varepsilon_r = 20.5$ and specified loss tangent $\tan\delta = 2 \times 10^{-5}$. Each single DR resonator has a dimension of $41 \times 41 \times 14$ mm^3 and the EM simulated Q factor is about 3600 where a conductivity of $\sigma = 2 \times 10^7$ S/m is assumed. The filter is routed in folded coupling topology with a target 20-dB return loss and two imaginary TZs for 60-dB rejection lobes on both the lower and upper rejection bands.

The whole tuning process takes 21 measurement and extraction steps by the VF-based CAT process. In each step, the tunable elements are incrementally adjusted by comparing the extracted circuit model with the target circuit model, and further adjustments are made based on the next extraction result (undershoot or overshoot). Since the extracted circuit model can accurately capture any change of each tuning element, the tuning result quickly converges to the target response. In this example, the filter responses of the first, second, fifteenth, and twenty-first tuning steps are shown in Fig. 4, where both the measurements

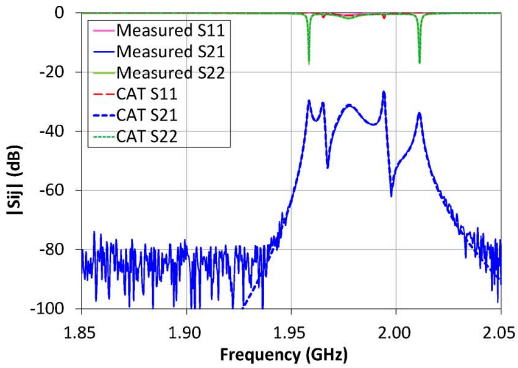

(a)

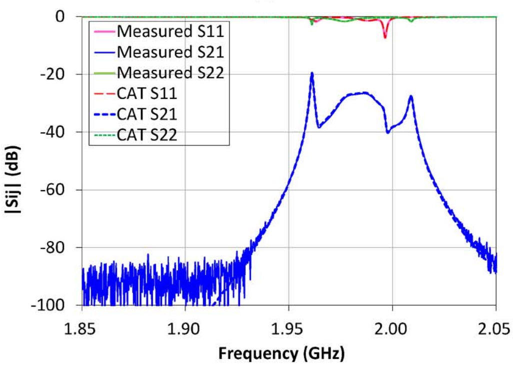

(b)

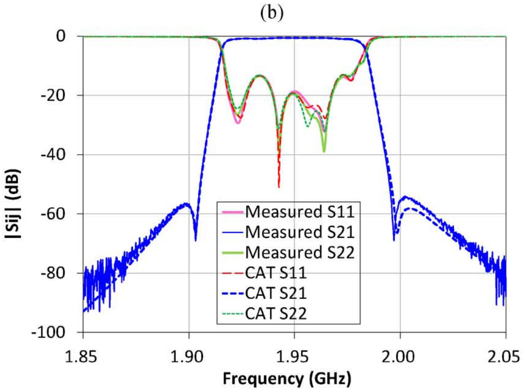

(c)

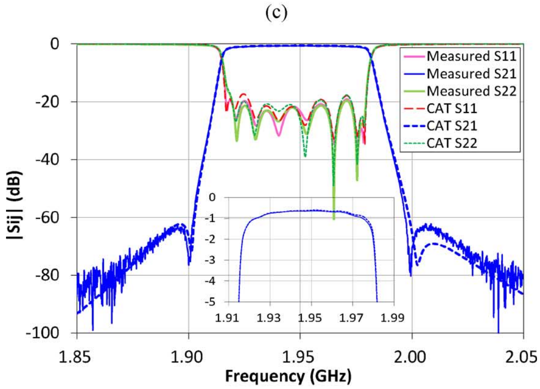

(d)

Fig. 4. S-parameter responses of the measurement and VF-CAT extracted models for the eight-pole TM dual-mode DR filter in different tuning states. (a) State 01. (b) State 02. (c) State 15. (d) State 21.

and the CAT results are compared. It can be seen that the two sets of curves in each tuning state agree very well with each other, even in the very initial states where the filter is severely detuned and under-coupled. The coupling values extracted for the four tuning states in Fig. 4 and the target coupling matrix are listed in

TABLE II
COUPLING VALUES CORRESPONDING TO THE FILTER STATES IN FIG. 4

	State 01	State 02	State 15	State 21	Target
M_{11}	-1.4803	-0.2487	0.0543	0.0520	0.0427
M_{22}	-1.0033	-1.1417	0.0148	0.0273	0.0468
M_{33}	-1.0897	-1.0840	-0.0155	0.0584	0.0443
M_{44}	-0.9397	-0.9000	-0.0196	0.0013	0.0131
M_{55}	-0.9466	-0.9591	0.1068	0.2223	0.2389
M_{66}	-1.3697	-1.3844	-0.1263	0.0202	0.0426
M_{77}	-1.0607	-1.0429	-0.0352	0.0280	0.0407
M_{88}	-1.4856	-1.4827	-0.0557	0.0385	0.0404
M_{S1}	1.1197	1.1830	0.9945	0.9965	0.9895
M_{12}	0.6067	0.6621	0.8676	0.8262	0.8281
M_{23}	0.0532	0.1673	0.6142	0.6118	0.5962
M_{34}	0.4496	0.4777	0.5520	0.5583	0.5497
M_{45}	0.0597	0.1186	0.6614	0.6173	0.6175
M_{56}	0.7155	0.6971	0.5585	0.5421	0.5383
M_{67}	0.3590	0.1316	0.6407	0.5988	0.5921
M_{78}	0.4621	0.4506	0.8566	0.8400	0.8305
M_{8L}	1.0072	0.9897	1.0065	1.0064	1.0079
M_{36}	-0.0995	-0.0519	-0.1635	-0.0826	-0.0846
M_{46}	-0.0313	-0.1059	-0.0500	-0.0986	-0.1000

TABLE III
UNLOADED Q FACTORS CORRESPONDING TO THE TUNING STATE 21

Q1	Q2	Q3	Q4	Q5	Q6	Q7	Q8
1769	2491	2756	2505	2796	2521	3579	1840

Table II. Since there always exists an equivalent spurious stray coupling M_{46} that accounts for the total stray coupling and dispersion effect, the target coupling matrix needs to be modified with the presence of the stray coupling by optimization. The stray coupling M_{46} in this example is called "equivalent" because its position is determined by the predefined complex rotation operations. The equivalent stray couplings are common to an analytical CAT technique for a practical filter tuning. Without taking them into account, the CAT process would not lead to the desired filter responses.

The extracted Qs of the filter at the final tuning state are shown in Table III, where the significantly low Qs for the first and last electric resonator are due to the loading effect of input/output structures. The varied Qs for each electric resonator are generally caused by the different tuning and coupling conditions of each electrical resonator and also the imperfect contact between the DR puck and the filter cavity walls. It is worth mentioning that in the initial states when the filter has a high insertion-loss level (>20 dB or so), the extracted Q factors will be inaccurate. However, when the tuning process approaches to the final states, the extracted Q factors will gradually converge and reflect the actual unloaded Qs for each resonator.

It can be seen the extracted and the target filter circuit models at the last state are very close to each other, demonstrating that the VF-based extraction algorithm can be applied to both the coarse and fine tuning of a practical microwave filter.

Example 2: Tuning an Eight-Pole Predistortion Filter

This example shows an adaptive design-and-tuning scheme of a predistortion TM dual-mode DR filter [20] with $f_0 = 1.951$ GHz and $\mathrm{BW} = 60$ MHz. The filter physical structure is the same as that in example 1, only smaller DR pucks with higher relative permittivity of $\varepsilon_r = 39$ are used.

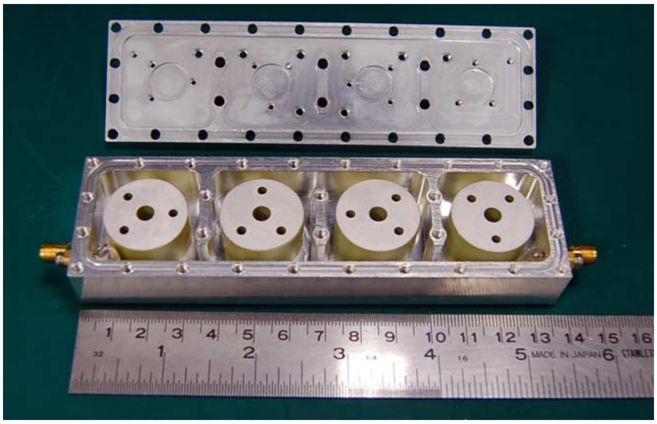

Fig. 5. Photograph of the prototyped eight-pole TM_{11} dual-mode DR filter. The dual-mode resonator is realized by DR pucks with $\varepsilon_r = 39$.

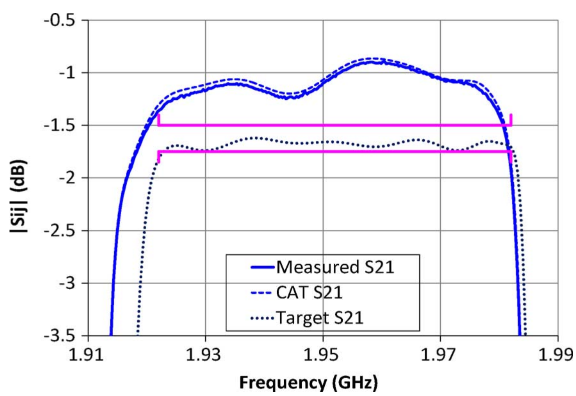

Fig. 6. Comparison of $|S_{21}|$ of the measured, targeted, and CAT results of the eight-pole predistortion filter at the initial tuning state. The solid pink lines (in online version) are the spec lines.

Each DR resonator has an inner size of $30 \times 30 \times 12$ mm^3, and the unloaded Q is about 2100. When the filter was prototyped into a conventional matched filter, the insertion loss at f_0 and the band edges are 0.85 and 2.2 dB, respectively. The filter hardware with top lid removed is shown in Fig. 5.

To achieve a predistortion filter characteristic with an effective filter Q of more than 10 000 in terms of the flatness of in-band insertion loss [11]–[13], the allowed in-band S_{21} ripple must be less than 0.25 dB, and the absolute level of the in-band insertion loss is as low as 1.7 dB.

Since in the beginning little is known about the actual Q factors of the DR resonators, an adaptive design-and-tuning scheme is proposed. The scheme begins with an initial target coupling matrix with a constant Q. Throughout the tuning process, the target coupling matrix is adaptively adjust by using the updated Qs from the previous tuning state. The details about the design-and-tuning scheme have been given in [20].

For this tuning example, a total of 12 extractions are made to realize the required 0.25-dB insertion-loss ripple. The responses at the initial tuning state of this predistortion filter are shown in Fig. 6, where it can be seen the CAT result closely matches the measured result. Since initially the filter is tuned from a matched condition, the in-band insertion loss is above the targeted level.

The results at the final tuning state are shown in Fig. 7. It can be observed that the CAT extracted model agrees very well with the measured data. The targeted and the extracted coupling matrices for the final tuning state are shown in Table IV, where the two circuit models are within a small error tolerance in terms of the coupling values. A threshold of 0.001 is used to screen out tiny couplings in the extracted model. The extracted Q factors of the filter at the final tuning state are listed in Table V. Clearly, the Q factors for each resonator are distinct, and the relative difference between Q1 and Q3 can be more than 100%. However, since the adaptive design-and-tuning scheme is used, the extracted Qs finally converge to the targeted Qs, and the finally achieved filter responses meet all the specs of a predistortion filter with an effective filter Q of 10 000.

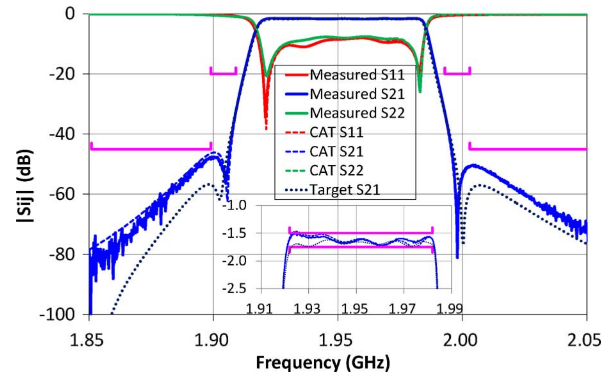

Fig. 7. S-parameters of the finally predistortion filter, where the in-band $|S_{21}|$ comparison is shown in the middle. The solid pink lines (in online version) are the spec lines.

TABLE IV
(A) Targeted Coupling Matrix at Final Tuning State. (B) Extracted Coupling Matrix at Final Tuning State

A

	S	1	2	3	4	5	6	7	8	L
S	0	1.1132	0	0	0	0	0	0	0	0
1	1.1132	0.0111	1.0373	0	0	0	0	0	0	0
2	0	1.0373	-0.0269	0.6570	0	0	0	-0.0039	0	0
3	0	0	0.6570	0.0119	0.638	0	-0.1190	0.0212	0	0
4	0	0	0	0.638	-0.145	0.5979	-0.1336	0	0	0
5	0	0	0	0	0.5979	0.3563	0.6186	0	0	0
6	0	0	0	-0.1190	-0.1336	0.6186	-0.1537	0.6648	0	0
7	0	0	-0.0039	0.0212	0	0	0.6648	0.2571	1.0261	0
8	0	0	0	0	0	0	0	1.0261	0.5136	1.1016
L	0	0	0	0	0	0	0	0	1.1016	0

B

	S	1	2	3	4	5	6	7	8	L
S	0	1.1205	0	0	0	0	0	0	0	0
1	1.1205	0.0238	1.0213	0	0	0	0	0	0	0
2	0	1.0213	0.0006	0.6502	0	0	0	0	0	0
3	0	0	0.6502	0.0196	0.6235	0	-0.1091	0.0224	0	0
4	0	0	0	0.6235	-0.1296	0.5882	-0.1592	0	0	0
5	0	0	0	0	0.5882	0.4022	0.5900	0	0	0
6	0	0	0	-0.1091	-0.1592	0.5900	-0.1937	0.6450	0	0
7	0	0	0	0.0224	0	0	0.6450	0.2737	1.0154	0
8	0	0	0	0	0	0	0	1.0154	0.4976	1.1135
L	0	0	0	0	0	0	0	0	1.1135	0

TABLE V
Unloaded Qs of the Predistortion Filter Final Tuning State

	Q1	Q2	Q3	Q4	Q5	Q6	Q7	Q8
Extracted	1109	1937	2827	1530	1191	2685	2320	1253
Target	1109	1972	2955	1548	1250	2620	2267	1314

VII. Conclusion

A vector-fitting-based analytical CAT technique, which can reliably and accurately determine the equivalent circuit model of a lossy microwave filter with an uneven-Q effect, has been proposed in this paper. The filter circuit model is constructed by the accurately extracted complex poles and residues of Y-parameters. It is proven that the complex residues in the Y-parameter fractional expansions must be considered when the uneven-Q effect is prominent. The way to deal with the complex poles and residues in order to extract the correct circuit model of a lossy filter has been presented. With this extraction technique, many challenging filter types, such as a high-order predistortion filter for an IMUX, can be effectively tuned. Two practical filter extraction examples given in this paper have demonstrated the effectiveness of this generalized analytical extraction method. It is believed that the proposed method can greatly enhance the efficiency of the research and development and mass production of the microwave bandpass filters.

REFERENCES

[1] R. J. Cameron, "Advanced coupling matrix synthesis technique for microwave filters," *IEEE Trans. Microw. Theory Techn.*, vol. 51, no. 1, pp. 1–10, Jan. 2003.

[2] A. E. Atia, A. E. Williams, and R. W. Newcomb, "Narrow-band multiple-coupled cavity synthesis," *IEEE Trans. Circuits Syst.*, vol. CAS-21, no. 5, pp. 649–655, May 1974.

[3] L. Accatino, "Computer-aided tuning of microwave filters," in *IEEE MTT-S Int. Microw. Symp. Dig.*, Jun. 1986, pp. 249–252.

[4] H. Hu and K.-L. Wu, "A deterministic EM design technique for general waveguide dual-mode bandpass filters," *IEEE Trans Microw. Theory Techn.*, vol. 61, no. 2, pp. 800–807, Feb. 2013.

[5] P. Harscher, R. Vahldieck, and S. Amari, "Automated filter tuning using generalized low-pass prototype networks and gradient-based parameter extraction," *IEEE Trans. Microw Theory Techn.*, vol. 49, no. 12, pp. 2532–2538, Dec. 2001.

[6] V. Miraftab and R. R. Mansour, "Computer-aided tuning of microwave filters using fuzzy logic," *IEEE Trans. Microw Theory Techn.*, vol. 50, no. 12, pp. 2781–2788, Dec. 2002.

[7] M. Yu and W.-C. Tang, "A fully automated filter tuning robots for wireless basestation diplexers," in *IEEE MTT-S Int. Microw. Symp. Comput.-Aided Filter Tuning Workshop*, 2003, (presentation).

[8] G. Macchiarella, "Extraction of unloaded and coupling matrix from measurement on filters with large losses," *IEEE Microw. Wireless Compon. Lett.*, vol. 20, no. 6, pp. 307–309, Jun. 2010.

[9] M. Meng and K.-L. Wu, "An analytical approach to computer-aided diagnosis and tuning of lossy microwave coupled resonator filters," *IEEE Trans. Microw. Theory Techn.*, vol. 57, no. 12, pp. 3188–3195, Dec. 2009.

[10] R. R. Mansour, "Filter technologies for wireless base stations," *IEEE Microw. Mag.*, vol. 5, pp. 68–74, Mar. 2004.

[11] R. M. Livingston, "Predistorted waveguide filters for use in communication systems," in *IEEE MTT-S Int. Microw. Symp. Dig.*, 1969, pp. 291–297.

[12] M. Yu, W.-C. Tang, A. Malarky, V. Dokas, R. J. Cameron, and Y. Wang, "Predistortion technique for cross-coupled filters and its application to satellite communication systems," *IEEE Trans. Microw Theory Techn.*, vol. 51, no. 12, pp. 2505–2515, Dec. 2003.

[13] A. Guyette, I. Hunter, and R. Pollard, "The design of microwave bandpass filters using resonators with nonuniform Q," *IEEE Trans. Microw. Theory Techn.*, vol. 54, no. 12, pp. 3914–3922, Dec. 2006.

[14] V. Miraftab and M. Yu, "Generalized lossy microwave filter coupling matrix synthesis and design using mixed technologies," *IEEE Trans. Microw Theory Techn.*, vol. 56, no. 12, pp. 3016–3027, Dec. 2008.

[15] R. J. Cameron, C. M. Kudsia, and R. R. Mansour, *Microwave Filters for Communication Systems*. Hoboken, NJ, USA: Wiley, 2007.

[16] B. Gustavsen and A. Semlyen, "Rational approximation of frequency domain responses by vector fitting," *IEEE Trans. Power Del.*, vol. 14, no. 3, pp. 1052–1061, Jul. 1999.

[17] B. Gustavsen, "Improving the pole relocating properties of vector fitting," *IEEE Trans. Power Del.*, vol. 21, no. 3, pp. 1587–1592, Jul. 2006.

[18] C. Liao, C. Chang, and J. Lin, "A vector-fitting formulation for parameter extraction of lossy microwave filters," *IEEE Microw. Wireless Compon. Lett.*, vol. 17, no. 4, pp. 277–279, Apr. 2007.

[19] H. Hu and K.-L. Wu, "A TM_{11} dual-mode dielectric resonator filter with planar coupling configuration," *IEEE Trans. Microw. Theory Techn.*, vol. 61, no. 1, pp. 131–138, Jan. 2013.

[20] H. Hu and K.-L. Wu, "An adaptive computer-aided design-and-tuning scheme for a predistorted filter with uneven-Q effect," in *IEEE MTT-S Int. Microw. Symp. Dig.*, Jun. 2013.

[21] R. A. Horn and C. R. Johnson, *Matrix Analysis*. New York, NY, USA: Cambridge Univ. Press, 1985.

Hai Hu (S'10–M'14) received the B.Sc. degree from Nanjing University, Nanjing, China, in 2004, and the M.Phil. and Ph.D. degrees in electronic engineering from The Chinese University of Hong Kong, Shatin, Hong Kong, in 2006 and 2013, respectively.

From 2006 to 2010, he was a Research Assistant with the Department of Electronic Engineering, The Chinese University of Hong Kong, where he was involved with numerical modeling of low-temperature co-fired ceramic (LTCC) layouts and passive integrated circuit components, automatic design of dual-mode waveguide filters, and manifold multiplexers for payload systems. In September 2013, he joined the Asia Satellite Telecommunications Company Ltd., Hong Kong, as a Senior Communications Systems Engineer. His research interests include microwave repeater system design and application for communication satellite payloads; analytical computer-aided tuning (CAT) techniques; computational electromagnetic (EM) algorithms for modeling of waveguide structures; and frequency- and time-domain numerical modeling and analysis of multilayered high-speed RF circuits.

Dr. Hu was the recipient of the 2012 Asia–Pacific Microwave Conference Prize.

Ke-Li Wu (M'90–SM'96–F'11) received the B.S. and M.Eng. degrees from the Nanjing University of Science and Technology, Nanjing, China, in 1982 and 1985, respectively, and the Ph.D. degree from Laval University, Quebec, QC, Canada, in 1989.

From 1989 to 1993, he was with the Communications Research Laboratory, McMaster University, as a Research Engineer and a Group Manager. In March 1993, he joined the Corporate Research and Development Division, COM DEV International, the largest Canadian space equipment manufacturer, where he was a Principal Member of Technical Staff. Since October 1999, he has been with The Chinese University of Hong Kong, Shatin, Hong Kong, where he is a Professor and the Director of the Radiofrequency Radiation Research Laboratory (R3L). He has authored or coauthored numerous publications in the areas of electromagnetic (EM) modeling and microwave passive components, microwave filters, and antenna engineering. His current research interests include partial element equivalent circuit (PEEC) and derived physically expressive circuit (DPEC) EM modeling of high-speed circuits, RF and microwave passive circuits and systems, synthesis theory and practices of microwave filters, antennas for wireless terminals, low-temperature co-fired ceramic (LTCC)-based multichip modules (MCMs), and RF identification (RFID) technologies. His research group is the main workforce in various active RFID research and applications in Hong Kong.

Prof. Wu is a member of the IEEE MTT-8 Subcommittee (Filters and Passive Components). He also serves as a Technical Program Committee (TPC) member for many prestigious international conferences including the IEEE Microwave Theory and Techniques Society (IEEE MTT-S) International Microwave Symposium (IMS). He was an associate editor for the IEEE TRANSACTIONS ON MICROWAVE THEORY AND TECHNIQUES (2006–2009). He was the recipient of the 1998 COM DEV Achievement Award for the development of exact EM design software of microwave filters and multiplexers and the Asia–Pacific Microwave Conference Prize in 2008 and 2012.